X-693-70-389

PREPRINT

NASA TM X-65374

TYPE III SOLAR RADIO BURST STORMS OBSERVED AT LOW FREQUENCIES

Part III Streamer Density, Inhomogeneities, and Solar Wind Speed

JOSEPH FAINBERG
R. G. STONE

OCTOBER 1970

GSFC
GODDARD SPACE FLIGHT CENTER
GREENBELT, MARYLAND

TYPE III SOLAR RADIO BURST STORMS OBSERVED AT LOW FREQUENCIES

Part III: Streamer Density, Inhomogeneities, and Solar Wind Speed

by

Joseph Fainberg and R. G. Stone
Radio Astronomy Branch
Laboratory for Extraterrestrial Physics
NASA-Goddard Space Flight Center
Greenbelt, Maryland

ABSTRACT

The analysis of a storm of type III solar radio bursts observed in August 1968 between 5 and 0.2 MHz by the RAE-I satellite has yielded the storm morphology, a possible relation to meter and decameter storms, and an average exciter speed of 0.37c between 10 and 40$R_\odot$ (Fainberg and Stone, 1970 a,b). A continuation of the analysis, based on the apparent dependence of burst drift rate on heliographic longitude of the associated active region, now provides a distance scale between plasma levels in the streamer, an upper limit to the scale size of coronal streamer density inhomogeneities, and an estimate of the solar wind speed. By fixing one

level the distance scale is utilized to determine the electron density distribution along the streamer between 10 and 40$R_\odot$. The streamer density is found to be 16 times that expected for the solar minimum quiet solar wind. An upper limit to the scale size of streamer density inhomogeneities is estimated to be of the order of 1 or 2 solar radii over the same height range. From the progressive delay of the central meridian passage (CMP) of the lower frequency emission, a streamer curvature is inferred which in turn implies an average solar wind speed of 380 km/sec between 14 and 36 $R_\odot$ within the streamer.

I. INTRODUCTION

The analysis of a storm of type III solar radio bursts has been continued. Previous work (Fainberg and Stone, 1970a, 1970b, hereinafter refered to as Paper I and Paper II) has been concerned with the storm morphology as well as a determination of the average burst exciter speed of 0.37c between 10 and 40 $R_{\odot}$. In this paper we discuss measurements of streamer density, inhomogeneities and solar wind speed.

With the exception of direct measurements by space probes between 0.7 and 1.5 A.U., our current knowledge of the interplanetary plasma beyond $10R_{\odot}$ comes from a variety of techniques such as the occultation of discrete radio sources by the solar corona, solar radar, the observation of comet tails, and the observation of type III solar radio bursts at long wavelengths. Newkirk (1967) has reviewed the structure of the solar corona and discusses many of these techniques further; Ness (1968) has reviewed the direct space probe measurements; and Brandt (1970) has

reviewed current work on the solar wind.

Yet most of the properties and structure within the vast range from 10 to 100$R_\odot$ remain to be investigated. Each of the techniques mentioned above has added some information, but also is limited in its application. Even the <u>in situ</u> measurements are frequently unable to discriminate between spatial and temporal characteristics. On the other hand, the scattering of radio waves by small density inhomogeneities in the corona leads to an increase in the apparent diameter of radio sources. If the scattering process were better understood, this promising method would provide detailed information about the structure and dynamic processes occuring in the corona. However, at the present time, there are still problems with the application of this method. Erickson (1964) derived an average electron density gradient between 10 and 80$R_\odot$ by utilizing the then available data and theory on scattering. The results derived in this way appear to give too large a density at

large distances as judged by comparison with direct measurements farther out.

The investigation of the interplanetary medium through the analysis of type III solar radio bursts at long wavelengths can in principal provide information about the structure and properties of active region streamers, which are the most prominent structures in the corona. But to investigate coronal heights above $10R_{\odot}$ by this method, the bursts must be observed at frequencies below 5 MHz, and consequently from above the ionosphere. All such observations have been conducted with antennas of low resolving power such as the short electrical dipole, so that in general the position of the emitting region cannot be directly observed. Assuming that the emission occurs at a frequency close to the plasma frequency of the medium in the streamer, the interpretation of dynamic spectra requires a model or at least additional assumptions. For example, if we assume a value of exciter speed, dynamic spectra can

yield the streamer electron density gradient along the path of the exciter, or conversely assuming the density gradient, the exciter speed can be inferred. These approaches have been applied by Hartz (1969), Alexander et al. (1969), Slysh (1967a), and Haddock and Graedel (1970) to the interpretation of satellite observations of solar bursts. Hartz (1969), for example, assumes a constant exciter speed and the distance of one plasma level. Alexander et al. (1969) invoke an energy density balance between the streamer and the ambient solar wind. This latter approach requires the use of a solar wind model, while the former approach depends on an assumed and constant exciter speed. It is interesting to note that the two approaches give similar results. Yet the required assumptions may leave the results open to criticism.

Assuming that the emission occurs at the plasma frequency, the main problem is the establishment of a distance scale. In view of the determination of a constant average exciter speed of 0.37c for the type

III storm events (paper II), a differential distance scale can be determined. However, as shown below, the same type of analysis which gives the exciter speed also provides a distance scale between plasma levels. We believe this evaluation of a differential distance scale in the 10 - 40$R_\odot$ height range is the most direct determination available thus far. This information will be used to obtain a density gradient along the streamer by fixing the height of one plasma level. But the distance between plasma levels is of itself important in the evaluation of the validity of various alternative theoretical models for the emission process , for example that proposed by Kuckes and Sudan (1969) or Slysh (1967b).

II. THE TYPE III STORM DATA

Since the morphology of a typical storm of type III bursts observed between 5 and 0.2 MHz by the RAE-I satellite has already been described in detail (papers I and II), only those features of importance for the present work will be reviewed. These storms,

which often persist for more than a complete solar rotation, are observable for at least a half solar rotation, i.e. the time required for the associated active region to move across the disc. Tens of thousands of drifting bursts are observed during this period and they are mostly of low intensity and of limited bandwidth. Both the burst occurence and apparent drift rates are a function of heliographic longitude, with both rates maximum near CMP and minimum near the limb position of the active region.

The apparent drift rate dependance is a consequence of the propagation time of the radio emission from the source position to the observer (paper II). Because of the large distances involved, this time is substantial, i.e. 23 seconds for free space propagation over a distance of 10 $R_{\odot}$. It is this phenomenon which, together with the large number of available bursts, forms the basis of the present work.

For the storm of August 1968, the analysis was based on 2500 bursts with clearly defined drift rates. The distribution of drift rates between

pairs of frequencies has been shown in the previous par's of this series of papers and will not be reproduced here. The least squares analysis (paper II) is based on the condition

$$\sum_m (t_{ji} - t_{ji}^m)^2 = \text{minimum}, \qquad (1)$$

where t_{ji}^m are the measured drift burst times between frequencies (and therefore plasma levels) i and j. The calculated drift time

$$t_{ji} = f(r_i, r_{ji}, \beta, t_s, t), \qquad (2)$$

where r_i is the distance from the sun to the higher frequency plasma level, r_{ji} is the distance between plasma levels, β is the exciter speed in units of c the speed of light, t_s is a reference time related to CMP, and t is the time. The very large number of bursts available for the least squares analysis provides a means of deriving the best fit values for r_i, r_{ji}, β, and t_s. The analysis, however, shows that the condition (1) is not sufficiently sensitive to

derive a best value for r_i over the range of available data ($r_i < 40R_o$) by the least squares procedure. For the first iteration, a reasonable value of r_i was chosen and the least squares procedure was used to fit r_{ji}, β, t_s. Later, a self consistent method based on the values of r_{ij} obtained over a wide frequency range was used to adjust values of r_i.

Necessary conditions for equation (1) are that

$$\frac{\partial}{\partial r_{ji}} \sum_m (t_{ji} - t_{ji}^m)^2 = 0,$$

$$\frac{\partial}{\partial \beta} \sum_m (t_{ji} - t_{ji}^m)^2 = 0, \text{ and} \qquad (3)$$

$$\frac{\partial}{\partial t_s} \sum_m (t_{ji} - t_{ji}^m)^2 = 0.$$

We have used equations (3) previously (paper II) to obtain β. In the implementation of the analysis, a guessed value and a correction term, such as $r_{ji} = r_{ji} + \delta_{ji}$ are used, and the correction term is determined from the analysis. After one calculation, the corrections are added to the guessed values and the procedure repeated. After 3 or 4 iterations,

the corrections become insignificant and values of r_{ji}, β, and t_s are obtained which do not depend on the original estimated value.

III. DISTANCE SCALE BETWEEN PLASMA LEVELS

The results of determining r_{ji}, the distance between plasma levels i and j, are summarized in Table I, along with the number of bursts used in the analysis and the frequencies corresponding to i and j.

TABLE I. DISTANCE BETWEEN PLASMA LEVELS r_{ji}

Frequency Interval MHz.	Derived Level Separation in Solar Radii	Adjusted Level Separation for Constant Exciter Velocity in Solar Radii	Number of Bursts
2.80-1.65	6.1	4.6	397
1.65-1.31	3.5	3.5	1497
1.31-0.995	4.4	4.5	847
0.995-0.700	6.0	6.9	250
0.700-0.540	19.4	9.8	77
2.80-1.31	10.0	8.4	272
2.80-0.995	15.2	12.9	131
1.65-0.995	7.9	8.0	614
1.31-0.700	10.2	11.3	172
1.65-0.700	11.4	14.7	128

The particular frequencies shown here correspond to

the fixed frequency radiometer channels for which the time resolution is 0.5 sec. The analysis will be extended over the entire frequency band from 5.4 to 0.2 MHz with smaller frequency intervals by using the swept frequency radiometer data from other receivers on RAE-I. The lower part of the table utilizes the same data but is calculated for larger frequency intervals to check the consistency of the results in the upper half of the table. In paper II the effect of sample size on the accuracy of the results was considered. It was shown that for less than two to three hundred bursts the possible errors increased rapidly. However, utilizing the value of β determined in paper II, a more accurate determination of r_{ji} is possible because it is primarily the ratio of β/r_{ji} which enters into the analysis. Therefore this has been utilized for the results shown in column 3 which are the adjusted level separations for a constant average β of 0.37c. It is clear that the values of r_{ji} derived in this way are close to the

values obtained without this adjustment when the number of bursts used in the analysis is large.

The assumptions involved in this analysis were discussed in paper II. First, it was assumed that the properties of the streamer and exciters were constant on the average over a half solar rotation. From the optical and high frequency radio observations of the active region during this period, this assumption seems reasonable. To confirm the assumption, the data were divided into sectors about CMP, and the analysis was carried out independently on each sector, showing essentially identical results. Secondly, any excess time due to group delay has been neglected on the assumption that the emission occurs in a density enhanced streamer and escapes to the ambient solar wind where the density is lower by a factor of the order of ten. The least squares analysis was also confined to data for heliographic longitudes less than 40^{o} about CMP to compare against the full 90^{o} heliographic longitude range. Again the results were

essentially the same suggesting that group delay effects could be neglected.

The level separations in Table I are used to obtain the electron density distribution along the streamer by fixing the absolute distance of any one plasma level. The choice of this level will determine whether there is an increase or decrease of streamer electron density enhancement above ambient levels with distance. In Figure 1 typical values of the coronal density for the quiet sun (Newkirk, 1967) are plotted. From 6 solar radii outward these values closely fit a power law of the form:

$$n_e = 3.45 \times 10^6 \, R^{-2.63} \quad (R > 6R_\odot). \qquad (4)$$

Using $11.6R_\odot$ as the level of 2.8 MHz emission and the level separations derived from the RAE data, we obtain a set of values which is plotted in Figure 1. The RAE values for this choice of starting level are closely approximated by a power law of the form:

$$n_e = 5.52 \times 10^7 \, R^{-2.63}, \qquad (5)$$

which is shown as the straight line through the RAE data points. This represents a streamer density enhancement of 16 times the quiet corona at solar minimum or about 8 times the quiet values near the current portion of the solar cycle. It should be noted that the most favorable conditions for the generation and escape of type III bursts are found in the densest regions of the streamer. In the Appendix, an analysis based on the variation of burst drift rates with frequency is given which lends weight to the above choice of 2.8 MHz emission level.

It is interesting to note that the streamer density obtained in this way is in agreement with that obtained by Hartz (1968) and Alexander et al. (1969).

IV. SCALE SIZE IN THE CORONA

For each pair of frequencies, the least squares analysis has yielded a best fit of the parameters of the theoretical model to the experimental drift times. A spread in the experimental drift times can result from a combination of spreads in exciter speeds,

exciter directions, and plasma density and from burst misidentifications. If we attribute this spread as due only to density fluctuations in the corona then we can get an upper bound on this scale size. Table II lists the average root mean square deviation of the experimental drift times from the theoretical model for the two-week storm period.

TABLE II. SPREAD IN DRIFT TIMES

Frequency Drift Range MHz	σ sec	$\beta\sigma$ $R_\odot$
2.8 - 1.65	8.4	1.3
1.65 - 1.3	5.5	0.9
1.3 - 1.0	6.9	1.1
1.0 - 0.7	11.5	1.8
0.7 - 0.54	14.0	2.2

Column 2 lists the standard deviation in seconds and column 3 lists this value in solar radii taking the exciter velocity as 0.37c.

Since the drift rate spread between two levels results from the density spread at each level we can obtain the spread at each level by taking $\frac{1}{\sqrt{2}}$ times

the values in Table II and averaging. These values are given in Table III.

TABLE III. SPREAD IN CORONAL LEVELS

Frequency MHz	Level $R_\odot$	Coronal Level Variation $R_\odot$	Scale Size $R_\odot$
2.8	11.6	$\pm$1.0	2
1.65	16.2	$\pm$0.8	1.6
1.3	19.7	$\pm$0.7	1.4
1.0	24.2	$\pm$1.0	2.0
0.7	31.1	$\pm$1.4	2.8
0.54	40.8	$\pm$1.6	3.2

Column 3 of this table represents the coronal level variation at each level necessary to account for the observed spread in burst drift rates. Column 4 lists the resulting scale sizes of 1.4 to 3.2 $R_\odot$.

These scale sizes are quite consistent with solar wind magnetic field fluctuations with correlation lengths of 2×10^6 km (Jokipii and Coleman, 1968) measured on Mariner IV. The RAE results are also consistent with the revised analysis of radio source

scintillations yielding correlation lengths of about 10^6 km (Jokipii and Hollweg, 1970).

V. SOLAR WIND SPEED BETWEEN 14 AND 36$R_\odot$

The determination of t_s from the condition contained in equations 3 shows that $t_s + 123^h.4$, the time of CMP as determined by the maximum drift rate, is a function of frequency and that t_s occurs later in time at the lower frequencies. These values are given in Table IV.

TABLE IV. TIME OF CMP

Frequency Interval MHz.	Mid Height Of Frequency Interval $R_\odot$	Time of CMP Passage UT August 20, 1968
2.80 -1.65	13.8	$5^h.2$
1.31 -0.995	21.6	$8^h.2$
0.700-0.540	36.0	$16^h.8$

If it is assumed that this progressive delay is caused by solar rotation (garden hose curvature) then this delay can be related to an average bulk velocity. If ΔR is the radial separation of two coronal emission

levels and ΔT is the delay in CMP, then $V_B = \Delta R/\Delta T$ where V_B is the average bulk speed between the levels. The data derived from the RAE observations are plotted in Figure 2 where the straight line represents an average bulk velocity of 380 km/sec for the streamer plasma between 14 and 36 $R_\odot$. The solid square on this figure is the CMP of the associated flare producing region (Sakurai and Stone, 1970).

A value of 380 km/sec for the solar-wind speed appears to be somewhat larger than would be anticipated from existing models for the average solar wind at distances between 14 and 36 $R_\odot$. However, recent work by Pneuman and Kopp (1970) on coronal energy transport processes indicates that the solar wind speed within a streamer should remain constant from 10 $R_\odot$ outward. On this basis, the RAE result at 14 - 36 $R_\odot$, which is typical of solar wind speeds measured at 1A.U., is quite reasonable.

With the availability of a still larger number of bursts, other storm events, and smaller frequency drift intervals, it will be possible both to refine these observations and to obtain the bulk speed at other times.

SUMMARY

The least squares analysis of 2500 type III storm bursts is based upon the heliographic dependence of the drift rate caused by the time of radio propagation from source to observer. The analysis provides, in addition to an average exciter speed of 0.37c, a distance scale between plasma levels in the 10 - 40 $R_\odot$ range, an inferred solar wind speed of 380 km/sec in the 14 - 36$R_\odot$ range, and an upper bound to the scale size of coronal inhomogeneities in the same height range.

APPENDIX

It is of interest to pursue a somewhat different analysis with the RAE data based on the variation of burst drift rate with frequency. We assume over the range of interest a power law variation of electron density N (in cm^{-3}) with solar altitude R (in solar radii $R_\odot$) along the path of the exciter:

$$N = N_o R^{-a}. \qquad \text{(A1)}$$

If we assume the type III bursts result from plasma excitation near the local plasma frequency by exciters traveling radially outward with velocity β (units of c), we can write an expression (Papagiannis, 1970) for the burst drift rate:

$$\frac{df}{dt} = - \frac{a\beta c}{2(1 - \beta \cos \theta) R_\odot (81 \times 10^{-6} N_o)^{\frac{1}{a}}} f^{\frac{a+2}{a}}, \qquad \text{(A2)}$$

where

c = velocity of light,

θ = angle of exciter direction to sun-earth line,

f = midpoint of frequency interval df.

For each day of the August storm, θ is approximately constant and we can determine the average drift rate from the RAE measurements and compare this with equation A2.

The data for August 24, 1968 are plotted in Figure 3. The straight line is the least squares fit to a power law with a slope a = 2.47 and $N_o = 3.2 \times 10^7$ particles/cm^3 (based on $\beta = 0.37$). Comparing this to equation 4 we see that this result is consistent with the density along the exciter paths on August 24 having a similar density slope as the quiet sun at solar minimum but enhanced in density by a factor of 9.

We have made a similar comparison for each of the days from August 12, 1968 to August 27, 1968. When these data are averaged we obtain the value a = 2.57

and an average enhancement by a factor of 21.

This result is quite consistent with the streamer having a constant enhancement over the average quiet sun values out to at least 40 $R_{\odot}$. It also lends weight to the choice of level for the 2.8 MHz radiation in section III and the resulting density scale in Figure 1.

REFERENCES

Alexander, J.K., Malitson, H.H., and Stone, R.G.: 1969, Solar Phys. 8, 388-397.

Brandt, J.C.: 1970, Introduction to the Solar Wind, W. H. Freeman Co, San Francisco.

Erickson, W.C.: 1964, Astrophys. J. 139, 1290-1311.

Fainberg, J. and Stone, R.G.: 1970a, Solar Phys. in press.

Fainberg, J. and Stone, R.G.: 1970b, Solar Phys. in press.

Haddock, F.T. and Graedel, T.E.: 1970, Astrophys. J. 160, 293-300.

Hartz, T.R.: 1969, Planet. Space Sci., 17, 267-287.

Jokipii, J.R. and Coleman, P.J.: 1968, J. Geophys. Res. 73, 5495.

Jokipii, J.R. and Hollweg, J.V.: 1970, Astrophys. J. 160, 745-753.

Kuckes, A.F. and Sudan, R.N.: 1969, Nature 223, 1048-1049.

Malitson, H.H. and Erickson, W.C.: 1966, Astrophys. J. 144, 337-351.

Ness, N.F.: 1968, Ann. Rev. Astron. Astrophys. 6, 79-114.

Newkirk, G., Jr.: 1967, Ann. Rev. Astron. Astrophys. 5, 213-266.

Papagiannis, M.D.: 1970, NATO Advanced Study Institute on the Physics of the Solar Corona, Athens, Greece.

Sakurai, K. and Stone, R.G.: 1970, Trans. Amer. Geophys. Union, 416.

Slysh, V.I.: 1967a, Kosm. Issled. 5, 867-910.

Slysh, V.I.: 1967b, Astron. Zn. 44, 487-489 (Soviet Astron. - A.J. 11, 389-391).

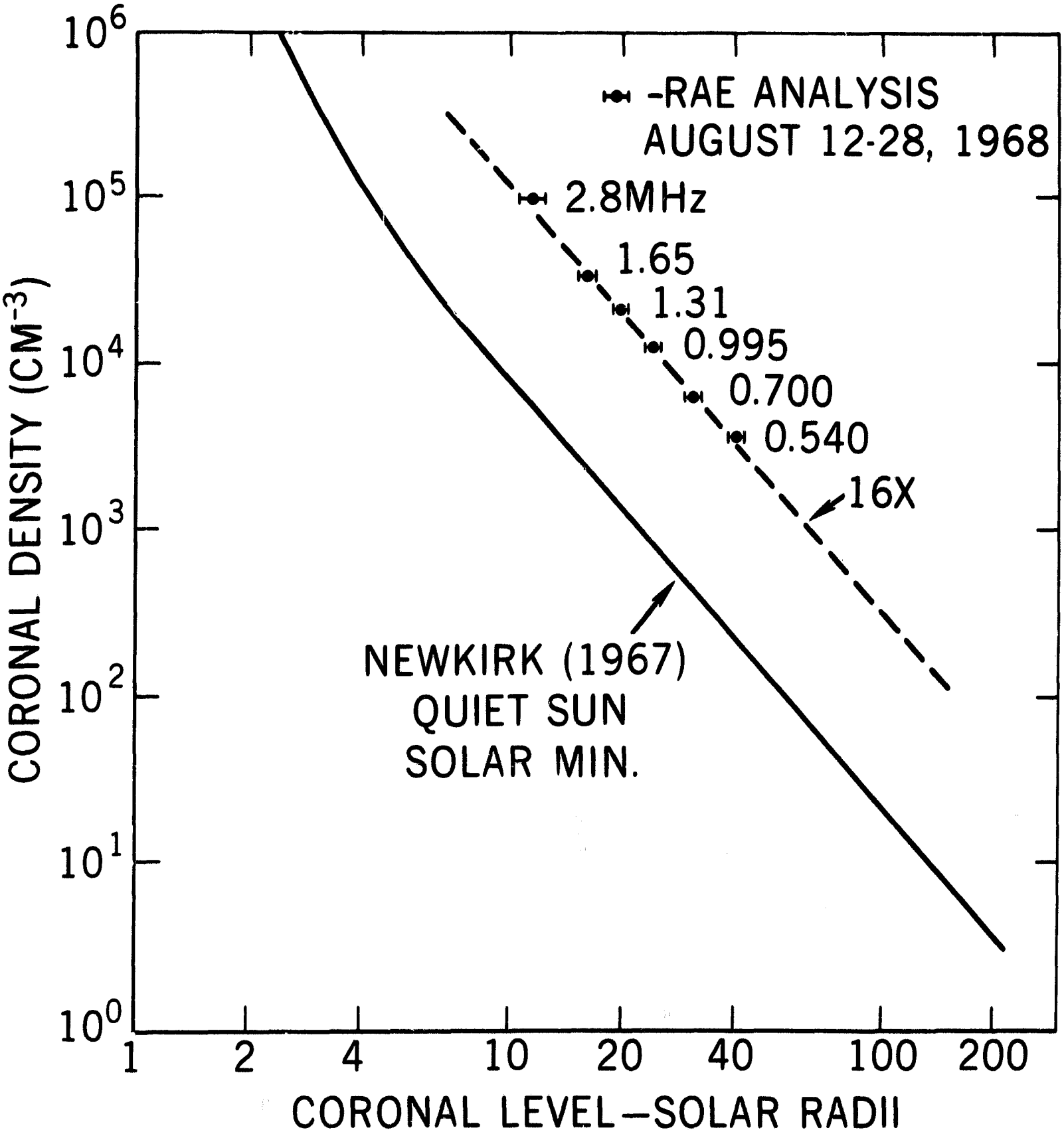

Figure 1 - Coronal density. The RAE values are plotted using 11.6 $R_\odot$ for the 2.8 MHz level and using the level separations derived from the least squares analysis of drift times for the other levels. The error bars are an upper bound to the inhomogeneity scale size as derived from a spread in the observed drift times.

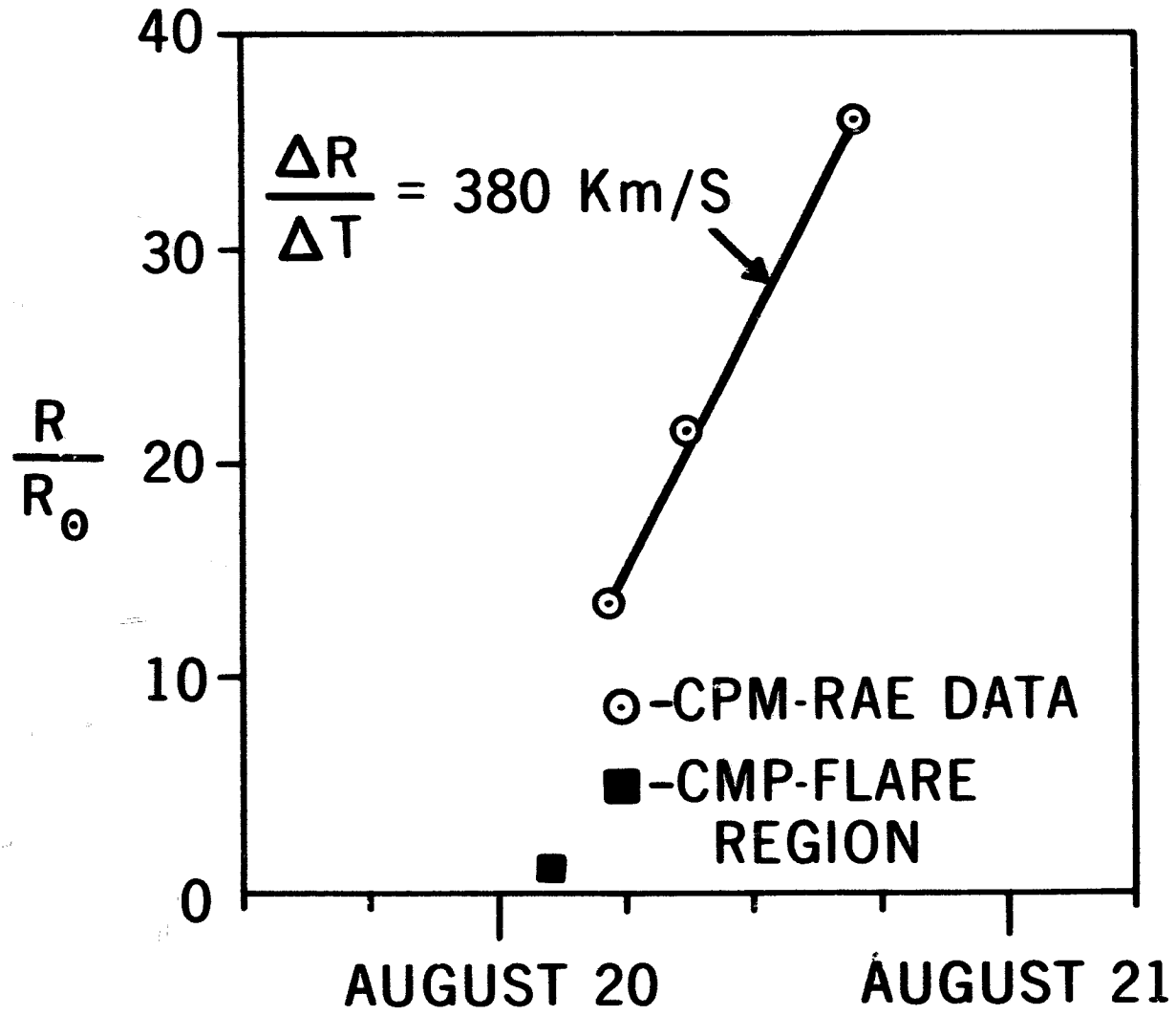

Figure 2 - Streamer solar wind speed. The RAE data points exhibit a progressive delay in CMP with distance implying an average bulk speed of 380 km/sec. The square represents the CMP for the associated flare region.

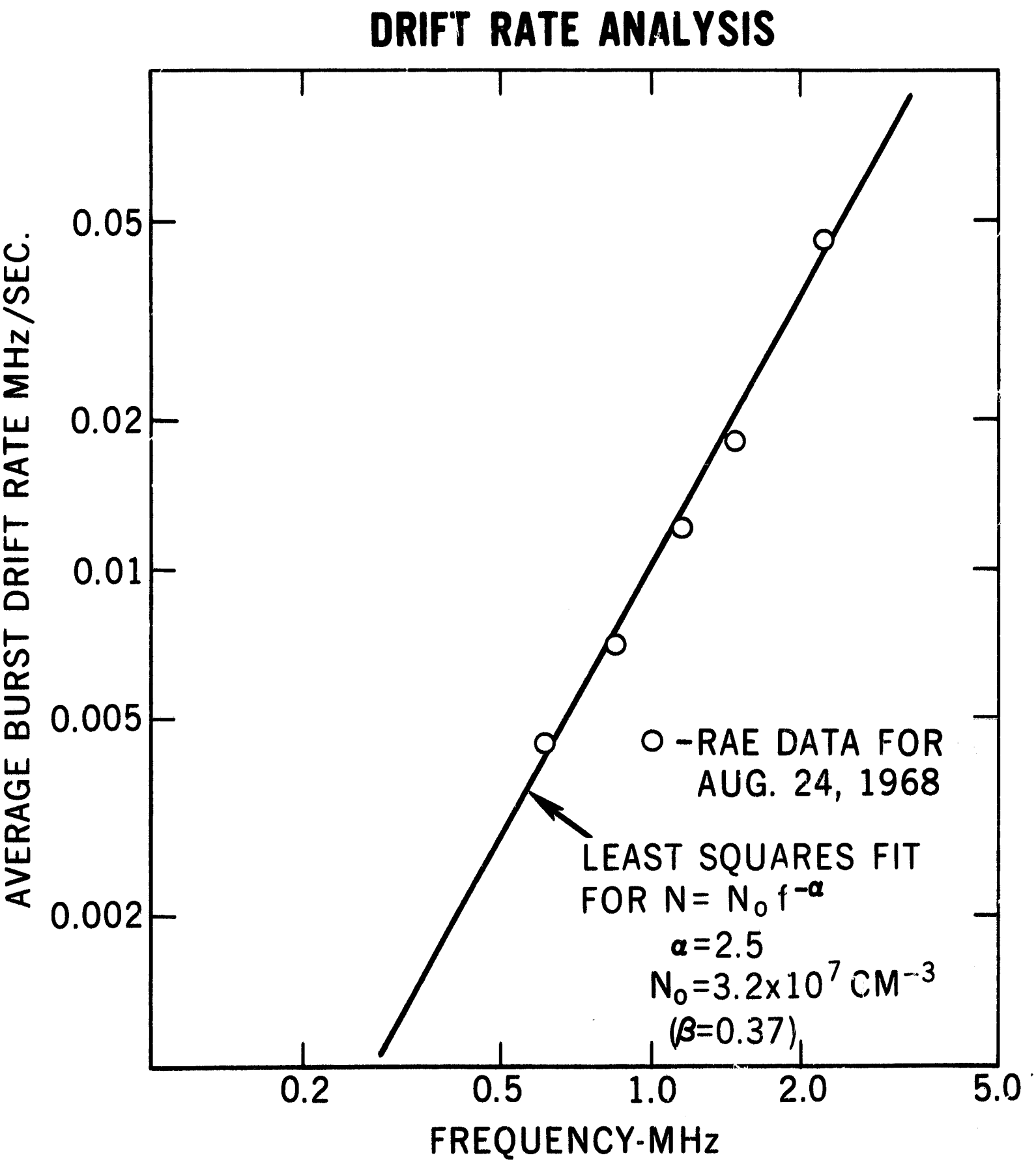

Figure 3 - Average burst drift rates for August 24, 1968 are plotted. The solid line is the least squares fit of the data to a power law dependence.